Published in the Proceedings of the 16th International Aluminum Alloys Conference (ICAA16) 2018
ISBN: 978-1-926872-41-4
by the Canadian Institute of Mining, Metallurgy & Petroleum

EFFECT OF Cr ADDITION ON MECHANICAL PROPERTIES AND MICROSTRUCTURE OF Al-Mn-Mg-Si ALLOYS

[*]Zhen Li[1,2], Zhan Zhang[1], X.-Grant Chen[1], and Hiromi Nagaumi[2]

1. Department of Applied Sciences, University of Québec at Chicoutimi, Saguenay, (Quebec), Canada, G7H 2B1

2. School of Iron and Steel, Soochow University, Suzhou, China, 215021
*(*Corresponding author: zhen.li1@uqac.ca)*

ABSTRACT

Recently, the remarkable strengthening effect of α-Al(Mn, Fe) Si dispersoids at both ambient temperature and elevated temperature were found by several researches. A large amount of dispersoids can be formed by applying special heat treatments and within a suitable range of chemical composition of AA3xxx alloys. In the present work, the influences of Cr addition on the mechanical properties and microstructures of the Al-Mn-Mg-Si alloys were investigated. The mechanical properties at ambient and elevated temperatures were evaluated by micro-hardness and yield strength. Moreover, the microstructures in as-cast and heat-treated conditions were quantitatively analyzed by optical and electron microscopes. Results revealed that Cr also had effect on the number density and volume fraction of dispersoids. Micro-hardness and yield strength at ambient temperature increased with the increasing content of Cr, and the Cr addition increased the yield strength at elevated temperature as well. Moreover, the creep resistance at 300°C improved dramatically with the increasing content of Cr.

KEYWORDS

AA3xxx alloys, Dispersoids, Cr, Mechanical properties at elevated temperature, Creep

INTRODUCTION

Traditionally, AA3xxx aluminum alloys were widely used in packaging, automobile and architecture industries, because of its good formability, excellent corrosion resistance and weldability. And AA3xxx alloys were considered as non-heat-treatable alloys. However, the strengthening effect of dispersoids in AA3xxx alloys was discovered recently (Li & Arnberg, 2003; Li, Muggerud, Olsen, & Furu, 2012; Li, Zhang, & Chen, 2016; Liu & Chen, 2015). A large amount of dispersoids could precipitate by a proper heat treatment.

In order to further improve AA3xxx alloys, the composition of the alloys should be optimized. A few previous studies were reported to investigate the influence of compositions on AA3xxx alloys. Adding Mn element could enhance the precipitation of α-Al(Mn, Fe)Si dispersoids and improve the yield strength (Muggerud, Mørtsell, Li, & Holmestad, 2013), as long as the concentration of Mn was under the solid solution limit. Fe decreased the solubility of Mn and accelerated the precipitation rate of α-Al(Mn, Fe)Si dispersoids(Li & Arnberg, 2003), the yield strength and creep resistance at elevated temperature could increase with an optimized content of Fe (Liu & Chen, 2016). Mg element would affect the nucleation process of α-Al(Mn, Fe)Si dispersoids by forming metastable Mg_2Si (Hirasawa, 1975; Li, Zhang, & Chen, 2017a; Lodgaard & Ryum, 2000), metastable Mg_2Si precipitated during heating process and promoted the precipitation of α-Al(Mn, Fe)Si dispersoids, moreover, Mg provided solid solution strength for AA3004 alloys (Li et al., 2016). Si increased the volume fraction of α-Al(Mn, Fe)Si dispersoids (Muggerud et al., 2013) and decreased the size of α-Al(Mn, Fe)Si dispersoids (Li, Zhang, & Chen, 2017b). With the addition of Mo, the size of dispersoids became finer with a higher volume fraction, the volume percentage of dispersoid free zones was reduced. Elevated temperature yield strength and creep resistance improved due to Mo addition (Liu, Ma, & Chen, 2017). However, the effect of Cr elements on microstructure and mechanical properties of AA3xxx alloys were rarely reported.

In the present study, the effect of Cr on microstructure and mechanical properties at room temperature and elevated temperature of Al-Mn-Mg-Si alloys were investigated. The microstructures are quantitatively evaluated by optical microscope and transmission electron microscope. The micro-hardness and yield strength at ambient temperature and elevated temperature were measured and creep tests at elevated temperature were also conducted.

EXPERIMENTAL PROCEDURES

Two alloys were designed to study the effect of Cr. The chemical compositions of these alloys were shown in Table 1. The content of Cr changed from 0 to 0.28%. These alloys were prepared by electric resistance furnace. The melt were maintained at 750°C for 30 minutes and degassed for 15 minutes. Then the melt were solidified in a permanent steel mold preheated at 250°C. The dimension of the ingot was 30 mm × 40 mm × 80 mm. In order to precipitate α-Al(MnFe)Si dispersoids, the samples were heated to 375°C with a 5°C/min heating rate. The holding time were from 2 to 24 h. Afterwards, the samples were water quenched to room temperature.

Table 1. Composition of DC series alloys (wt. %)

Alloy code	Cr	Mn	Fe	Mg	Si	Al
DC0	**0**	1.23	0.60	0.97	0.24	Bal
DC30	**0.28**	1.23	0.62	1.05	0.23	Bal

Vicker hardness were measured with a 200 g load and a 20 s dwelling time. 10 measurements were performed at the polished samples to obtain the average value of each sample. Compression yield strength tests were conducted at 25 and 300°C by a Gleeble 3800 thermomechanical simulator unit with a strain rate of 0.001 s^{-1}. The Gleeble samples were machined in a cylinder form with 15 mm in the length and 10mm in the diameter. Three measurements were conducted to get the average values. Compression

creep tests were performed at 300°C for 96 h with 58 MPa load. Each creep test was repeated twice. The creep samples were the same size as the Gleeble samples.

Optical microscope and scanning electron microscope were used to observe the as-cast and heat-treated microstructures. In order to reveal dispersoid free zone of α-Al(Mn,Fe)Si (DFZ) clearly, the polished samples were etched by 0.5% HF for 25 seconds. The volume fraction of intermetallic particles and DFZ were quantified by image analysis software (Clemex PE 4.0) with polished samples. TEM foils were prepared by twin-jet machine using a solution of 30% nitric acid in methanol at –25°C. Transmission electron microscope (TEM, JEM-2100) operated at 200 kV was used to observe the precipitation behavior dispersoids. An electron energy loss spectroscope (EELS) attached to the TEM was used to measure the thickness of the samples. The volume fraction of dispersoids was calculated according to the method introduced in previous literature (Li & Arnberg, 2003) shown in Eq. (1):

$$V_{\mathrm{v}} = A_{\mathrm{A}} \frac{\mathrm{K}\bar{\mathrm{D}}}{\mathrm{K}\bar{\mathrm{D}} + \mathrm{t}} (1 - A_{\mathrm{DFZ}}) \quad (1)$$

Where A_{A} is the volume percentage of the dispersoid zone, A_{DFZ} is the volume percentage of the DFZ, $\bar{D}$ is the average equivalent diameter of the dispersoids, t is the TEM foil thickness, and K is the average shape factor of dispersoids, which was 0.45 (Li & Arnberg, 2003).

RESULTS AND DISCUSSION

As-Cast Microstructure

Figures 1a and 1b were the as-cast microstructure of DC series alloys. Two types of intermetallic particles presented in all these alloys. The black particles were primary Mg_2Si and the grey color particles were Mn-containing intermetallics. For base alloys, DC0 alloys, the grey color phases were Al_6(Mn, Fe) intermetallic particles. However, Cr elements were detected in the grey phases of DC30 alloys according to EDS results as shown in Figure 2. These phases were identified as Al_6(Mn, Fe, Cr) intermetallics. The volume fraction of primary Mg_2Si and Mn-containing intermetallic particles were measured as well. The quantitative results were shown in Table 2. The volume fraction of primary Mg_2Si were not affected by the addition of Cr elements. On the other hand, because of the addition of Cr, the volume fraction of Mn-containing intermetallic particles increased from 3.6% to 4.6%. This was due to the addition of Cr which formed Al_6(Mn, Fe, Cr) intermetallic particles.

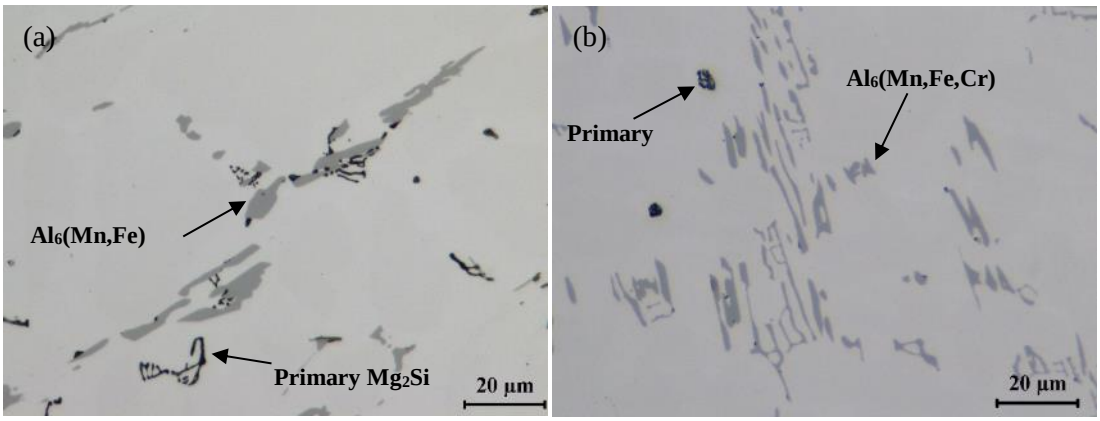

Figure 1. As-cast microstructure of (a) DC0 alloys and (b) DC30 alloys

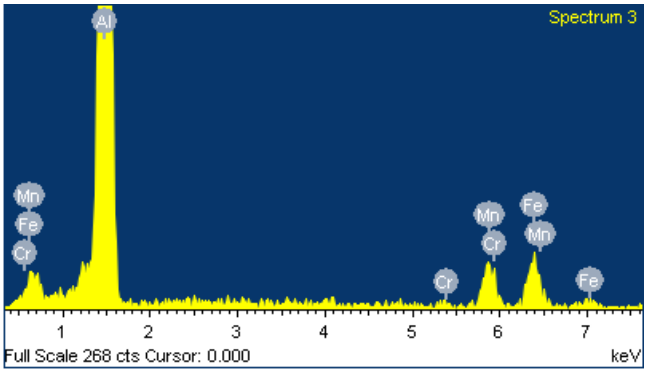

Figure 2. The EDS spectrum of Mn-containing intermetallic particles

Table 2. Volume fraction of Mn-containing intermetallic particles and primary Mg_2Si of as-cast condition

Alloy code	**DC0**	**DC30**
Mn-containing intermetallic (%)	3.67	4.54
Primary Mg_2Si (%)	0.11	0.12

Dispersoid Zone and Dispersoid Free Zone

After heat-treatment at 375°C for 24 h, a large amount of dispersoids precipitated in DC0 alloys and DC30 alloys. But due to the small size of dispersoids, they could not be observed by optical microscope. In order to observe the distribution of dispersoids, the alloys were etched by 0.5%HF for 25 s. Then two types of microstructure could be observed as shown in Figures 3a and 3b. The areas with darker color were defined as dispersoid zone. Within dispersoid zone, large number density of dispersoids were found according to TEM observation of previous literature (Li & Arnberg, 2003; Li et al., 2017b; Liu & Chen, 2015). On the other hand, the light color areas were defined as dispersoid free zone (DFZ). This was due to low number density of dispersoids inside dispersoid free zone. By analyzing dispersoid zone and dispersoid free zone, the distribution of dispersoids in large scale could be evaluated. In the present study, the distribution of dispersoid free zone and dispersoid zone were very similar for all these three alloys. Dispersoid free zone presented around intermetallic particles and along grain boundaries. Moreover, according to the quantitative results as shown in Table 3, the volume fraction of dispersoid zone slightly decreased due to the addition of Cr element.

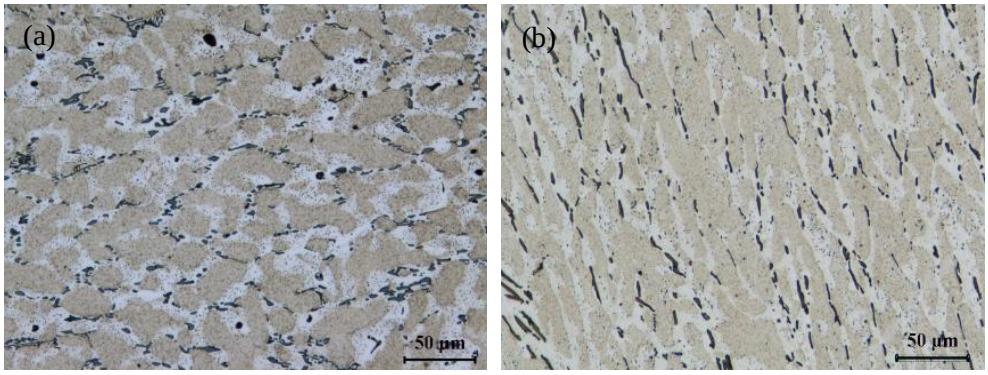

Figure 3. After heat-treatment at 375°C for 24 h, dispersoid zone and dispersoid free zone of (a) DC0 alloys and (b) DC30 alloys

Table 3. After heat-treatment at 375°C for 24 h, volume fraction of dispersoid zone and dispersoid free zone (DFZ)

Alloy code	**DC0**	**DC30**
Dispersoid zone (%)	69.69	66.59
Dispersoid free zone (%)	26.45	29.41

Dispersoids

In order to observe the morphology of dispersoids, transmission electron microscope (TEM) had to be used due to the small size of dispersoids. After heat-treatment at 375°C for 24 h, a large amount of dispersoids precipitated in both DC0 alloys and DC30 alloys as shown in Figures 4a and 4b. The shape of the dispersoids in these two alloys was quite similar, which was also consistent with previous literature (Li et al., 2016; Muggerud, Walmsley, Holmestad, & Li, 2015). In Cr-free DC0 alloys, the dispersoids could be identified as α-Al(Mn, Fe) Si dispersoids based on the shape and composition, which agreed with many previous work (Li & Arnberg, 2003; Li et al., 2012; Liu & Chen, 2015, 2016; Muggerud et al., 2013). However, in DC30 alloys, a small amount of Cr element were detected in the dispersoids according to the EDS results as shown in Figure 5. So the dispersoids in DC30 alloys could be identified as α-Al(Mn, Fe, Cr) Si dispersoids.

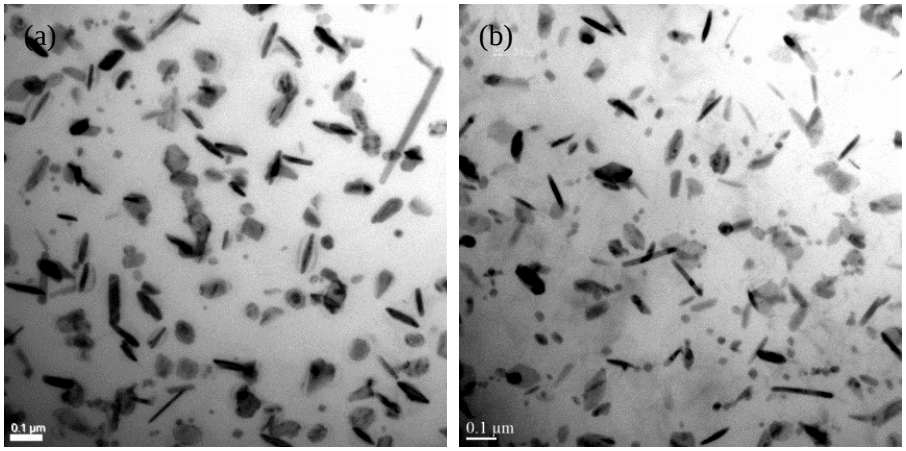

Figure 4. After heat-treatment at 375°C for 24 h, the morphology of dispersoids in (a) DC0 alloys and (b) DC30 alloys

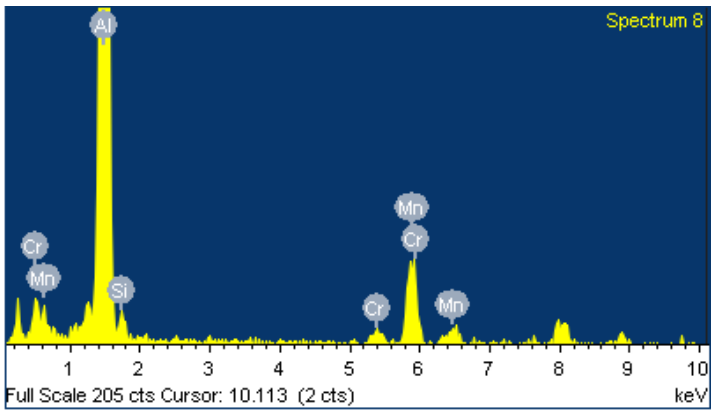

Figure 5. The EDS spectrum of α-Al(Mn, Fe, Cr) Si dispersoids precipitated in DC30 alloys

As shown in Table 4, the equivalent diameter, number density and volume fraction of dispersoids were quantitatively analyzed based on TEM images. The equivalent diameter of dispersoids in DC0 alloys and DC30 alloys were both around 50 nm. But the number density of dispersoids dropped from 1054.94 to 607.14 μm^{-3} caused by Cr addition. Finally, the decrement of number density leaded to the loss of volume fraction of dispersoids. The volume fraction of dispersoids of DC0 alloys and DC30 alloys were respectively 2.69% and 1.80%. DC30 alloys possessed less dispersoids than DC0 alloys. This may be due to the volume fraction increment of intermetallic particles in DC30 alloys. As shown in Table 2, the volume fraction of Mn-containing intermetallic particles increased from 3.67 to 4.54% because of Cr addition. Moreover, these intermetallic particles were insoluble at 375°C. Therefore, the available content of solute Mn element for the precipitation of dispersoids decreased.

Table 4. Volume fraction of dispersoids in DC0 alloys and DC30 alloys

Alloy code	**DC0**	**DC30**
Equivalent diameter (nm)	49.80	47.44
Number density (1/μm^3)	1054.94	607.14
Volume fraction (%)	2.69±0.36	1.80±0.31

Electrical Conductivity and Micro-Hardness

Electrical conductivity of DC0 alloys and DC30 alloys were measured to evaluate the solute element level. The results are shown in Figure 6a. While the heat-treatment holding time increased, the electrical conductivity of DC0 alloys and DC30 alloys first climbed sharply then increased slowly. The electrical conductivity of DC30 alloys was lower than DC0 alloys. Based on the EDS test results (Figures 2 and 5), only a small amount of Cr element found in the intermetallic particles and dispersoids. It indicated that most of Cr element were still in solid solution.

Figure 6b was the results of micro-hardness after holding at 375°C from 2 h to 48 h. For both DC0 alloys and DC30 alloys, the micro-hardness evolution curves were very similar. At first, the hardness kept increasing sharply until the holding time reached 12 h. Then, as the holding time increased, the hardness increased slightly. The tendency of micro-hardness curve were very similar with electrical conductivity curve. The peak hardness was achieved by holding at 375°C for around 24 h. And DC30 alloys which were with 0.3% Cr addition had a higher hardness than Cr-free DC0 alloys.

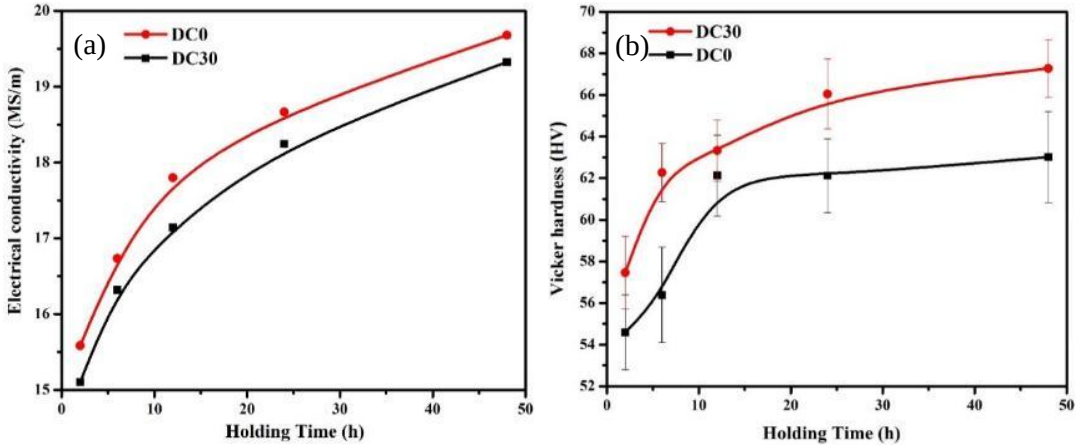

Figure 6. (a) Electrical conductivity and (b) Micro-hardness as a function of holding time at 375°C

Yield Strength at 25°C and 300°C and Creep Resistance at 300°C

After heat-treatment at 375°C for 24 h, the yield strength of DC0 alloys and DC30 alloys were measured at both 25 and 300°C. The results were respectively shown in Figure 7a and 7b. The room and elevated temperature yield strength of DC0 alloys were 97.5 and 81.2 MPa. And for DC30 alloys, the yield strength measured at 25 and 300°C were 105.8 and 82.8 MPa, respectively. With 0.3% Cr addition, yield strength at 25 and 300°C increased 8.3 and 1.6 MPa, respectively.

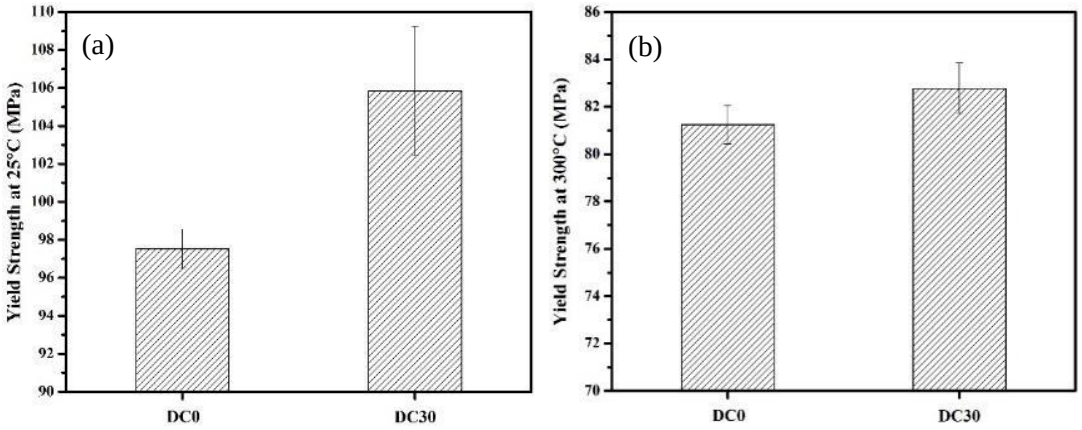

Figure 7. After heat-treatment at 375°C for 24 h, compression yield strength results (strain rate0.001 s^{-1}) of DC0 alloys and DC30 alloys at (a) 25°C and (b) at 375°C

Moreover, in order to evaluate materials' elevated temperature mechanical properties, compression creep resistance tests were also conducted at 300°C. The creep curves were shown in Figure 8. After holding at 300°C with 58 MPa load for 96 h, the strain of DC0 alloys and DC30 alloys were 0.25 and 0.025, respectively. The materials' creep resistance at elevated temperature improved dramatically because of 0.3% Cr addition.

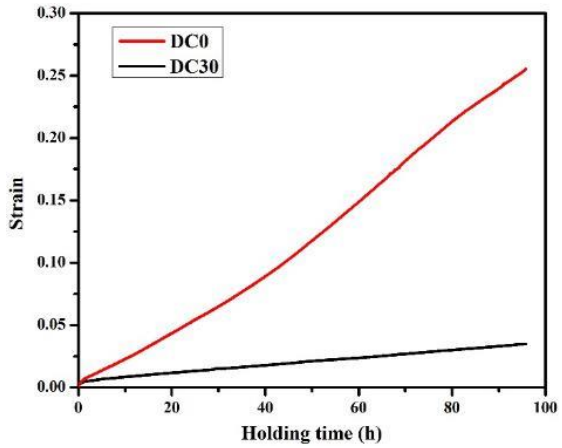

Figure 8. After heat-treatment at 375°C for 24 h, the creep curve measured at 300°C for 96 h with 58 MPa load of DC0 and DC30 alloys

It was well known that dispersoids were the key strengthening phases for AA3xxx alloys at both room and elevated temperature (Li et al., 2017b; Liu & Chen, 2015; Muggerud et al., 2013). But in the present study, the volume fraction of dispersoids decreased due to Cr addition (Table 4). However, the room and elevated temperature strength of materials increased as Cr content increased. It indicated that the

effect of Cr for present study was not on dispersoid strengthening. On the other hand, very small amount of Cr element found in the intermetallic particles and dispersoids. It mean that most of Cr element were still in solid solution. Therefore, Cr addition mainly strengthened materials by solid solution strengthening.

CONCLUSIONS

- The volume fraction of Mn-containing intermetallic particles increased with the content of Cr element.
- Cr element was found in α-Al(Mn, Fe, Cr) Si dispersoids. However, the number density and volume fraction of dispersoids decreased due to the addition of Cr.
- Micro-hardness at 25°C, yield strength at 25°C and at 300°C, creep resistance measured at 300°C increased with Cr addition. This was caused by the solid solution effect of Cr.

REFERENCES

Hirasawa, H. (1975). Precipitation process of Al-Mn and Al-Cr supersaturated solid solution in presence of age hardening phases. *Scripta Metallurgica, 9*(9), 955-958. https://doi.org/10.1016/0036-9748(75)90551-7

Li, Y. J., & Arnberg, L. (2003). Quantitative study on the precipitation behavior of dispersoids in DC-cast AA3003 alloy during heating and homogenization. *Acta Materialia, 51*(12), 3415-3428. https://doi.org/10.1016/S1359-6454(03)00160-5

Li, Y. J., Muggerud, A. M. F., Olsen, A., & Furu, T. (2012). Precipitation of partially coherent α-Al(Mn,Fe)Si dispersoids and their strengthening effect in AA 3003 alloy. *Acta Materialia, 60*(3), 1004-1014. https://doi.org/10.1016/j.actamat.2011.11.003

Li, Zhen, Zhang, Zhan, & Chen, X. Grant. (2016). Effect of magnesium on dispersoid strengthening of Al—Mn—Mg—Si (3xxx) alloys. *Transactions of Nonferrous Metals Society of China, 26*(11), 2793-2799. https://doi.org/10.1016/S1003-6326(16)64407-2

Li, Zhen, Zhang, Zhan, & Chen, X. Grant. (2017a). Effect of metastable Mg_2Si and dislocations on α-Al(MnFe)Si dispersoid formation in Al-Mn-Mg 3xxx alloys. *Submitted to Materials Characterization*.

Li, Zhen, Zhang, Zhan, & Chen, X. Grant. (2017b). Microstructure, elevated-temperature mechanical properties and creep resistance of dispersoid-strengthened Al-Mn-Mg 3xxx alloys with varying Mg and Si contents. *Materials Science and Engineering: A, 708*(Supplement C), 383-394. https://doi.org/10.1016/j.msea.2017.10.013

Liu, K., & Chen, X.-G. (2016). Evolution of Intermetallics, Dispersoids, and Elevated Temperature Properties at Various Fe Contents in Al-Mn-Mg 3004 Alloys. *Metallurgical and Materials TransactionS B, 47*(6), 3291-3300. https://doi.org/10.1007/s11663-015-0564-y

Liu, K., & Chen, X. G. (2015). Development of Al–Mn–Mg 3004 alloy for applications at elevated temperature via dispersoid strengthening. *Materials & Design, 84*, 340-350. https://doi.org/10.1016/j.matdes.2015.06.140

Liu, K., Ma, Hezhaoye, & Chen, X. Grant. (2017). Enhanced elevated-temperature properties via Mo addition in Al-Mn-Mg 3004 alloy. *Journal of Alloys and Compounds, 694*, 354-365. https://doi.org/10.1016/j.jallcom.2016.10.005

Lodgaard, Lars, & Ryum, Nils. (2000). Precipitation of dispersoids containing Mn and/or Cr in Al–Mg–Si alloys. *Materials Science and Engineering: A, 283*(1–2), 144-152. https://doi.org/10.1016/S0921-5093(00)00734-6

Muggerud, Astrid Marie F., Mørtsell, Eva Anne, Li, Yanjun, & Holmestad, Randi. (2013). Dispersoid strengthening in AA3xxx alloys with varying Mn and Si content during annealing at low temperatures. *Materials Science and Engineering: A, 567*, 21-28. https://doi.org/10.1016/j.msea.2013.01.004

Muggerud, Astrid Marie F., Walmsley, John C., Holmestad, Randi, & Li, Yanjun. (2015). Combining HAADF STEM tomography and electron diffraction for studies of α-Al(Fe,Mn)Si dispersoids in 3xxx aluminium alloys. *Philosophical Magazine, 95*(7), 744-758. https://doi.org/10.1080/14786435.2015.1006294